

CERTAIN PROPERTIES OF SPECTRALLY INTEGRATED
AND SPECTRAL TRANSMITTANCES OF FRESHWATER ICE
FROM 400-700 NM

S.J. Bolsenga Great Lakes Environmental Research
 Laboratory
 Ann Arbor, MI 48105-1593 USA

ABSTRACT

Considerable information is available on the transmittance of photosynthetically active radiation (PAR: 400-700 nm) through sea ice, whereas relatively little is known about PAR transmittance through freshwater ice. Transmittances of PAR through some common freshwater ice types (including clear ice, refrozen slush, and snow ice) are reported from studies using instruments which measure both spectral (2-10 nm increments) and spectrally integrated transmittances over this range. Snow causes the greatest attenuation of radiation, often reducing transmittances to 10% or less over the spectrum as a result of even light covers (2-8 cm). Clear ice showed transmittances of 80-95% for the spectrally integrated data and from 65 to nearly 95% for the spectral data. Transmittances of other ice types were bounded by the clear ice/snow-covered-ice transmittance range. Comparisons between the spectral and spectrally integrated data sets show specific applications for each type of measurement.

1. INTRODUCTION

Information on the transmittance of incident photosynthetically active irradiance (PAR: 400-700 nm) through sea ice is plentiful. Some of these studies have combined ice optics with under-ice ecology (e.g. Maykut and Grenfell, 1975; Perovich et al, 1986; Palmisano et al, 1987; Sookhoo et al, 1987) while others have included only sea ice optics (Grenfell and Maykut,

1977; Gilbert and Buntzen, 1986; Grenfell and Perovich, 1986). Similar studies on the transmittance of PAR through freshwater ice are not as numerous and not nearly as well advanced. Recent studies, using quality sensors, include Maguire, 1975a,b and Bolsenga, 1978 and 1981. Many early freshwater ice studies used substandard sensors and methods which render the results questionable. The sea ice studies cited above have used spectroradiometers to measure incident and transmitted radiation, whereas the freshwater studies have used instruments which measure incident and transmitted radiation integrated over the 400-700 nm range. This paper summarizes and highlights the more important properties of the integrated freshwater ice transmittance measurements and provides some new spectral transmittance data collected with a scanning underwater spectroradiometer. The measurements are from both large and small freshwater lakes including, and in the geographical area of, the North American Laurentian Great Lakes. The results compare the two types of measurements (integrated and spectral), discuss their relative usefulness, and project possible future research with respect to freshwater ice transmittance.

2. INSTRUMENTATION & METHODS

Two separate instrumentation systems were used: radiation sensors consisting of topside and underwater quantum sensors (hereafter called the "integrated sensor"), which measured radiation integrated over the PAR spectrum; and an underwater scanning (400-850 nm) spectroradiometer for spectral measurements. All of the sensors were manufactured by the Li Cor Corporation (Lincoln, Nebraska USA). Measurements reported in this paper were made at a distance of about 2 cm under the ice bottom. Measurements at greater depths will be reported elsewhere.

The underwater quantum sensor was light and required only an "L-shaped" arm fabricated from 3.2 cm diameter white plastic pipe, liberally perforated for ease in submerging, to carry the sensor (Figure 1). The sensor was located approximately 80 cm from the borehole and was adjustable to a level position which could be checked topside by an above-ice spirit level. A platform equipped with three large screws was used to hold and level the arm.

The suspension device for the heavy (25 kg in air) underwater

spectroradiometer consisted of sections of 5.1 cm diameter aluminum pipe for vertical control and a hinged member to move the instrument to an

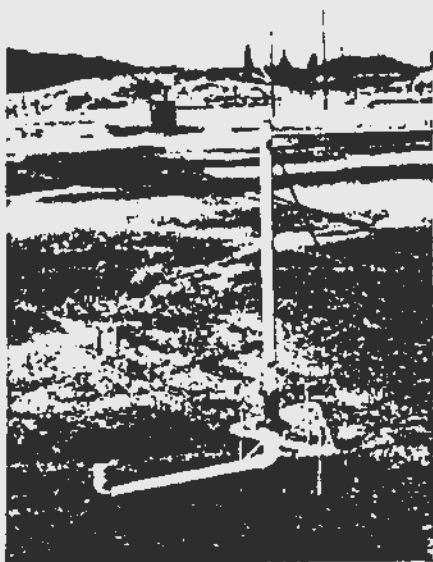


Figure 1. The L-shaped arm used to support the integrated sensor (400-700 nm). Depth of the arm was adjusted for ice thickness by means of a slip-joint on the vertical member.



Figure 2. The underwater spectroradiometer with buoyancy floats, horizontal folding arm, and vertical depth-adjustment member.

undisturbed area 2 m away from an access hole in the ice (Figure 2). The spectroradiometer was guided under the ice to the full length of the arm and the vertical member locked into a surface tripod (Figure 3). Floats attached to the instrument provided neutral buoyancy. The instrument was



Figure 3. The tripod securing the vertical member of the spectroradiometer system.

attached to the horizontal arm by a shackle which allowed free horizontal movement for automatic leveling. Neutral buoyancy and leveling were achieved prior to field operations in a laboratory tank. Vertical movement to acquire readings at various depths was accomplished to a depth of 5 m by adding additional sections of measured and marked pipe; at greater depths the unit was lowered by marked line. Typically a scan was taken in air, at depths of approximately 2 cm under the ice and at 1, 2, 3, 5, and 10 m under the ice surface, and at the bottom. The sequence was repeated in reverse with a scan in air completing the operation. Total

time for a complete operation varied from 7-10 min. During that time, uniform sky conditions, as indicated by visual observations and by the beginning and ending air scans were required. Scans were not used where changing sky conditions accounted for variability of greater than 3-4% in the repeat transmittance values at various depths.

3. TRANSMITTANCES

Transmittances are reported for clear ice, snow covered ice, refrozen slush, and white ice (refrozen slush, snow ice)-clear ice combinations (Table 1). Clear ice showed the highest transmittances of all the ice types measured. However, the amount of radiation penetrating a given ice cover varied widely depending on the type of clear ice measured (crack and bubble structure) and the cloud cover. The transmittances vary from 0.70 to 0.95 for the integrated sensor (Table 1, Cases 1,2) with the average transmittances of the spectral values (Cases 3,4) falling within that range (0.79-0.87). Cloud cover influenced clear ice transmittances significantly. In one situation, the integrated sensor was positioned under 36 cm of clear ice (Case 2). Under clear skies, two ratios of 0.95 were obtained. At the same site on the following day when 10/10ths cloud cover prevailed during the entire period, the ratios remained in a narrow 0.70 - 0.76 range. Figure 4 shows two clear ice spectral data sets. Even though the top ice layer of the sample for Trace 1 exhibited extensive bubble structure (Table 1, Case 3, Note b), the transmittances remained above 0.70 throughout most of the spectral range. Skies were clear during the measurements and the average transmittance (0.87) compares favorably with the integrated clear sky measurements. Trace 2 in Figure 4 shows transmittances through another clear ice location (Table 1, Case 4) with stippled surface. The values are about 3-10% lower than the ice in Trace 1 likely because the stippled surface affords more of a diffuse reflector than the surface in Trace 1.

A snow cover of just a few centimeters in depth attenuates most of the incoming radiation to an underlying ice surface. Measurements were made at two locations where snow-covered and snow-free clear ice were located in the same area (Table 1; Cases 1,5; and Cases 4,8). Using the integrated sensor under a 3 cm snow cover (Case 5), ratios of transmitted to incident radiation were reduced by over 70% from the snow-free surface (Case 1). Comparison of average transmittances of the snow covered vs.

Table 1. Case number (C), sensor type, ice type and thickness, integrated sensor transmittance (T), maximal transmittance of spectral sensor (Max T), maximal transmittance wavelength (λ), and average spectral transmittance from 400-700 nm.

C	Sensor	Ice Type/Thickness(cm)	T	Max T, λ (nm)	Avg T
Clear Ice					
1)	Integ	Clear/28 (a)	0.77-0.89		
2)	Integ	Clear/36	0.70-0.95		
3)	Spect	Clr + semi clr(b)/25.5+8(c)		0.94 (560)	0.87
4)	Spect	Clear/21 (d)		0.86 (542)	0.79
Snow Covered Ice					
5)	Integ	Snw cvd/28+3 (a)	0.09-0.12		
6)	Integ	Snw cvd/37+2+1 (e)	0.18		
7)	Integ	Snw cvd/43+3+1 (f)	0.17		
8)	Spect	Snw cvd/21+7-8 (d)		0.03 (564)	0.01
White Ice					
9)	Integ	Refroz slush/27	0.15-0.31		
Clear/White Ice Combination					
10)	Integ	Clr + ref slsh/38+4	0.58		
11)	Integ	Clr + ref slsh/37+2	0.66		
12)	Spect	Clr + wht ice/6.5+18		0.54 (570)	0.47
13)	Spect	Clr + snw ice/13+7		0.52 (562)	0.50

(a) 3 cm wind-packed snow over one area, 0 cm snow nearby. Measurements from same borehole;

(b) Clear ice is classified as having few bubbles and cracks. The semi clear ice contained a dense structure of evenly distributed elongated bubbles oriented perpendicular to the ice surface;

(c) Stratigraphy from bottom to top layers for all cases;

(d) Clear ice with stippled surface, 7-8 cm snow over one area, 0 cm snow nearby. Measurements from same borehole.

(e) 37 cm clear ice, 2 cm refrozen slush, 1 cm new snow;

(f) 43 cm clear ice, 3 cm refrozen slush, 1 cm granular metamorphosed snow.

snow-free ice as measured by the spectroradiometer shows a nearly 80% reduction in transmittance (Table 1; Cases 4,8; Figure 4; Traces 2,3). Maximal transmittances shifted 22 nm higher for the snow covered ice. To further illustrate the effect of snow on PAR transmittance, snow was removed from the ice/snow combination listed in Table 1, Case 6. The ratio of under-ice to above-ice radiation rose from 0.18, with undisturbed snow, to 0.66, with the snow removed.

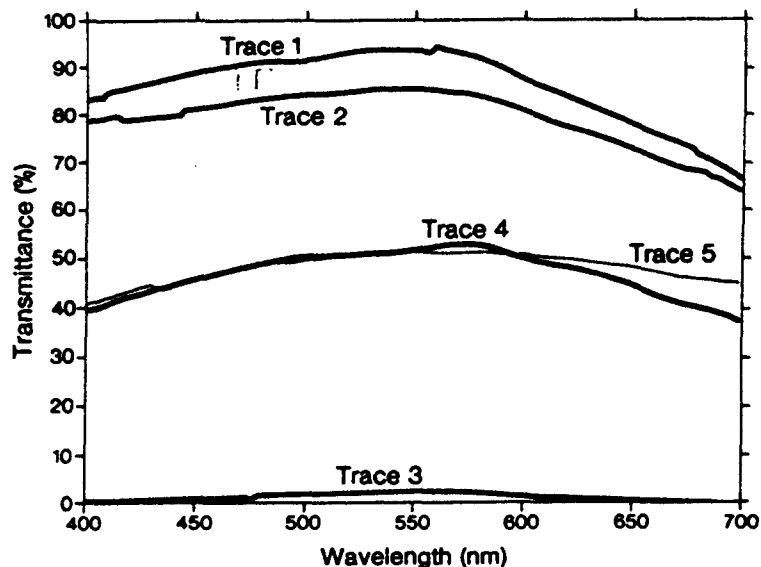


Figure 4. Spectral transmittances through 33.5 cm of clear ice with the top 8 cm exhibiting an extensive bubble structure (Trace 1); through 21 cm of clear ice with a stippled surface (Trace 2); and the same 21 cm of clear ice covered by 7-8 cm of snow (Trace 3). Spectral transmittances of 18 cm of white ice over 6.5 cm of clear ice (Trace 4) and 7 cm of snow ice over 13 cm of clear ice (Trace 5).

The term white ice includes the more specific ice types snow ice and refrozen slush. Snow ice forms from upward water seepage through stress cracks in an existing ice cover loaded with a snow layer, which subsequently refreezes. Refrozen slush forms with mild temperatures or

rain which reduce a snow cover to slush, which subsequently refreezes. Only one measurement of an ice cover composed completely of white ice, in this case refrozen slush, is available (Table 1, Case 9). Measurements with the integrated sensor showed transmittance ratios which varied depending on the bubble content and albedo of the ice with lower transmittances obtained in an area of higher ice albedo. Measurements of clear/white ice combinations are shown in Table 1 (Cases 10-13) and Figure 4 (Traces 4 & 5). Average transmittances of the spectral measurements, are consistent with transmittances from the integrated sensor, taking into account differences in stratigraphy.

Extinction coefficients, k (cm^{-1}), for representative integrated sensor values in this study and from Maguire (1975a,b) are:

Clear ice 0.0006 to 0.02 ± 0.003 ;

Combinations of clear ice, white ice, snow 0.027 to 0.059 ;

Snow, new soft 0.10 ± 0.02 ;

Snow, hard powder 0.500 ± 0.05 .

4. DATA APPLICATIONS AND FUTURE STUDIES

4.1 Spectrally integrated data

In a recent under-ice ecology program (Bolsenga et al. 1988), PAR at the air/water and ice/water interfaces was estimated, using a limited number of on-site measurements and many of the previously collected measurements described above with some surprising results (Bolsenga and Vanderploeg, 1989). The site was a large (162 km^2 surface area) bay of Lake Michigan, USA before, during, and after ice cover. Incident total solar radiation was measured approximately 35 km from the measurement site. Incident PAR was computed from an empirical equation. To compute the amount of PAR entering the water column through snow and ice, the ice types, amount of snow on the ice, their general abundance and location, and the position of the ice edge were observed from the surface (aircraft or satellite imagery could have been used); ice thickness and stratigraphy were measured. Observations of snow and ice-type, abundance, and location were collected by an individual with experience in measuring PAR transmittance through similar types of ice and ice-snow combinations making assignment of

estimated transmittance values as accurate as possible. Transmittances were then weighted according to the areal coverage of each type.

The estimated transmittances during February and March (months with ice cover) were higher than expected for two reasons: 1) larger amounts of clear, snow-free ice over the bay than expected, and 2) both ice cover months included periods of open water. The lack of snowcover was caused by high winds blowing snow from the surface and by above freezing temperatures and rain for a portion of the ice-covered period. Figure 5 shows that even though the transmittances during ice cover decreased significantly, transmitted PAR does not show the precipitous decreases measured on many small, heavily snow-covered lakes. In addition, high monthly incident PAR during the ice-covered months, compared to the open-water months, contributes to the smooth transition in transmitted PAR from fall to winter to spring. Without high incident PAR, transmitted PAR during the ice-covered months would have exhibited a significant decrease, but not as much as would be expected for a many north temperate inland lakes which are normally totally snow-covered.

It is unlikely that much additional work on spectrally integrated PAR transmittance is warranted for the ice types and thicknesses already examined. The existing information enables experienced observers to estimate the PAR transmittance of large or small areas from minimal data such as snow thickness and extent, ice thickness, type, and coverage. In areas with ice conditions dissimilar to those already measured, additional study would be required to provide the baseline data necessary for reasonably accurate estimates.

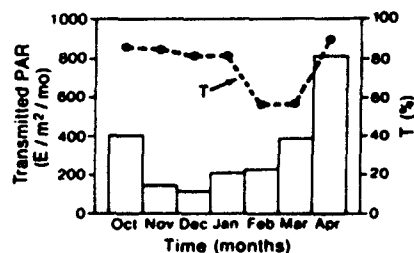


Figure 5. Transmittances (T) and transmitted PAR estimated for an under-ice ecology pilot program.

4.2 Spectral data

One principal application for spectral data is with detailed under-ice ecology programs. Such studies will almost always require on-site, spectral data since varying atmospheric conditions, metamorphosis of the ice/snow surfaces, and variable stratigraphy of the ice from location to location will affect the depth of the biota as well as their horizontal location. Freshwater zooplankton often adjust their position in the water column according to both the quantity and wavelengths of radiation available. Estimates of spectrally integrated PAR as described above will continue to be useful for pilot studies and large area estimates of PAR transmittance, but detailed studies such as those in the polar regions as described in the introduction will continue to use on-site, spectral measurements. It is possible that fiber optic probes could be used. Some speculation exists, for example, that light penetration in canded ice covers is considerably higher along crystal boundaries (Bolsenga et al., 1989), thus creating favorable environments for the biota in those concentrated areas.

5. ACKNOWLEDGMENT

Mr. David Norton of the Great Lakes Environmental Research Laboratory designed and fabricated the instrument support systems and assisted in the measurements. GLERL Contribution # 650.

6. REFERENCES

- Bolsenga, S.J. and H.A. Vanderploeg. 1989. Estimating photosynthetically active irradiance to open and ice-covered freshwater lakes: Methods and preliminary results, submitted for publication.
- Bolsenga, S.J., J.E. Gannon, G. Kennedy, D.C. Norton, and C.E. Herdendorf. 1989. ROV Dives Under Great Lakes Ice. *Cold Regions Science and Technology*. 16:89-93.
- Bolsenga, S.J., H.A. Vanderploeg, M.A. Quigley, and G.L. Fahnenstiel. 1988. An under ice ecology pilot program, operations and preliminary scientific results. *Journal of Great Lakes Research* 14:372-76.

- Bolsenga, S.J. 1981. Radiation transmittance through lake ice in the 400-700 nm range. J. Glaciol. 27:57-66.
- Bolsenga, S.J. 1978. Photosynthetically active radiation transmission through ice. NOAA Technical Memorandum ERL GLERL-18, Boulder, Colo.
- Gilbert, G.D. and R.R. Buntzen. 1986. In-situ measurements of the optical properties of arctic sea ice. SPIE Vol. 637, Ocean Optics VIII: 252-263.
- Grenfell, T.C. and G.A. Maykut. 1977. The optical properties of ice and snow in the Arctic basin. Journal of Glaciology 18:445-463.
- Grenfell, T.C. and D.K. Perovich. 1986. Optical properties of ice and snow in the polar oceans. II: Theoretical calculations. SPIE Vol. 637, Ocean Optics VIII:242-251.
- Maguire, R.J. 1975a. Effects of ice and snow cover on transmission of light in lakes. Inland Waters Directorate, Canada Centre for Inland Waters, Tech. Bull. No. 54:6.
- Maguire, R.J. 1975b. Light transmission through snow and ice. Inland Waters Directorate, Canada Centre for Inland Waters, Tech. Bull. No. 91:4.
- Maykut, G.A. and T.C. Grenfell. 1975. The spectral distribution of light beneath first-year sea ice in the Arctic Ocean. Limnology and Oceanography 20:554-563.
- Palmisano, A.C., J.B. SooHoo, R.L. Moe, and C.W. Sullivan. 1987. Sea ice microbial communities. VII. Changes in under-ice spectral irradiance during the development of Antarctic sea ice microalgal communities. Mar. Ecol. Prog. Ser. 35:165-173.
- Perovich, D.K., G.A. Maykut, and T.C. Grenfell. 1986. Optical properties of ice and snow in the polar oceans. I: Observations. SPIE Vol. 637, Ocean Optics VIII:232-241.
- Roulet, N.T. and W.P. Adams 1984. Illustration of the spatial variability of light entering a lake using an empirical model. Hydrobiologia, Vol. 67, No. 74, pp. 67-74.
- SooHoo, J.B., A.C. Palmisano, S.T. Kottmeier, M.P. Lizotte, S.L. SooHoo, and C.W. Sullivan. 1987. Spectral light absorption and quantum yield of photosynthesis in sea ice microalgae and a bloom of *Phaeocystis pouchetii* from McMurdo Sound, Antarctica. Mar. Ecol. Prog. Ser. 39:175-189.
- Stewart, K.M. and B.E. Brockett. 1984. Transmission of light through ice and snow of Adirondack lakes, New York. Verh. Internat. Verein. Limnol., Vol. 22, pp. 72-76.

FRACTURE TOUGHNESS OF S2 COLUMNAR FRESHWATER ICE: CRACK LENGTH AND SPECIMEN SIZE EFFECTS - PART II

J.P. Dempsey
Associate Professor

Y. Wei and S. DeFranco
Research Assistants

R. Ruben and R. Frchetti
NSF Undergraduate Trainees

Department of Civil and
Environmental Engineering
Clarkson University
Potsdam, NY 13676

U.S.A.

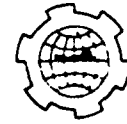
ABSTRACT

Wedge loaded compact tension (WLCT) specimens were tested to investigate the influence of both crack length and specimen size versus grain size on the fracture toughness of S2 columnar freshwater ice. For one grain size and one specific crack orientation, the crack length was varied as a function of the grain size, ranging over a major portion of the length of the specimen. The crack length effects on the critical-energy-release-rate (G_{1c}) were studied in this way for three specimen sizes. Two parallel research efforts have already been completed using S2 ice but different loading configurations (Bentley et al., 1988; Dempsey et al., 1989). These previous studies and this study allow preliminary observations to be made concerning the influence of specimen size and the comparative merits of the energy approach. The overall objective is to obtain a criterion for the minimum dimension in terms of grain size in order for small scale yielding conditions to apply.

1 INTRODUCTION

In this study, reproducible values for critical toughness corresponding to the initiation of a stationary macrocrack are sought. In this context it is assumed that prior to loading no previous crack growth has occurred. Following crack initiation, the crack motion or propagation must be essentially planar. Assuming that the crack-microstructure orientation is kept fixed, and that the geometrical dimensions of the test specimen are "large enough" with respect to the microstructure (so that the assumptions of continuum mechanics are valid), then the value of K_1 (the stress intensity factor) or G_1 (the energy release rate) at which a stationary macrocrack extends in a given material should be independent of the size and shape of the test specimen and the method of loading. The value obtained for the fracture toughness could then be regarded as a material property.

An approach that is directly meaningful for anisotropic materials is one in which the



POAC 89

The 10th International Conference
on Port and Ocean Engineering
under Arctic Conditions.
June 12-16 1989, Luleå, Sweden

VOLUME 1

Edited by

K.B.E Axelsson L.Å. Fransson

Department of Civil Engineering
Luleå University of Technology
Luleå, Sweden